Absorption Waves Produced by CO_2 Laser Ablation

H.-A. Eckel*, J. Tegel, W.O. Schall

German Aerospace Center (DLR) – Institute of Technical Physics, Stuttgart, Germany

ABSTRACT

A requirement for efficient pulsed laser propulsion from ground to LEO is the achievement of a specific impulse of up to 800 s at a jet efficiency of at least 50%. With CO_2 laser radiation at pulse lengths in the range of 10 microseconds and polymers as propellant these numbers cannot be attained by classical laser ablation because the impulse formation by laser ablation is limited by the premature absorption of the incident laser radiation in the initially produced cloud of ablation products[1, 2]. The power fraction of a CO_2 laser pulse transmitted through a small hole in a POM sample has been compared with the incident power. It was found that the transmitted power fraction is directly proportional to the inverse of the pulse energy. The plasma formation in vacuum and in air of 3500 Pa and the spread of the shock wave with velocities of 1.6 to 2.4 km/s in the low pressure air was observed by Schlieren photography. A sharp edged dark zone with a maximum extension of 10 to 12 mm away from the target surface develops within 5 µs independently of the pressure and is assumed to be a plasma. In order to find out, if this is also the zone where the majority of the incident laser radiation is absorbed, a CO_2 probe laser beam was directed through the expansion cloud parallel to and at various distances from the sample surface. The front of the absorption zone is found to move rapidly away from the target surface with increasing speed. The absorption lasts twice as long as the laser pulse. It is not associated with a pressure rise that would increase the mechanical impulse. The radial motion of the absorption wave turned out to be faster than the shock wave seen in the Schlieren pictures.

Keywords: Laser propulsion, plasma diagnostics

1. INTRODUCTION

The efficiency of the ablation of solid polymers for the production of impulses under various conditions has been studied intensively for CO_2 laser pulses of pulse lengths between 12 and 15 µs. Flat samples have been irradiated with fluence values ranging from 22 to 150 J/cm^2 [2,3]. The values cover the region designated optimum for the attainable coupling coefficient [4]. Measurements of the laser power arriving on the sample surface as a function of the incident laser pulse energy have indicated severe energy losses in front of the target. The source for these losses not only reduces the arriving energy in magnitude but also shortens the length of the efficative pulse on the target surface [3]. It is well known, that in experiments with pulsed laser ablation a breakdown of the air or of ablated material in front of the target occurs by Inverse Bremsstrahlung and launches a laser supported detonation wave that moves away from the surface. In this wave much of the laser pulse energy may be captured, preventing further ablation and hence the production of impulse by conservation of momentum.

The proof of the existence and the knowledge of the position of an emerging laser absorption wave in front of the surface is imperative for the understanding of the obvious losses of laser energy. The absorption process may not only be a function of the fluence on the target, but also of the pulse length and hence the intensity.

The understanding and observation of the on-going processes requires the application of short-time measurement techniques. A simple and cheap method is the transsection of the region of the vapor and plasma region with one or several CO_2 probe beams in combination with fast detectors. The measurement with beams at various distances from the target surface can render information on the local appearance, the lifetime and the optical thickness of absorbing media at every location and thus detect even moving absorption waves. In combination with a shadowgraphic or Schlieren type of visualization of the flow field, valuable insight should be gained into the prevailing processes and the character of the laser initiated absorption wave.

*hans-albert.eckel@dlr.de; Dr. Hans-Albert Eckel, DLR- Institut für Technische Physik, Postfach 80 03 20, 70503 Stuttgart, Germany; phone +49 711 6862 714; fax +49 711 6862 788

2. EXPERIMENTAL SETUP

The arrangement of the CO_2 pulse laser and the measurement of pulse energy and power has been described in previous publications, including the measurement setup for the power transmitted through a 3 mm diameter hole in the target samples [3]. With a few exceptions of PVN, the sample material was in all cases either plain POM or POM with 20% of aluminum powder, as used in previous investigations.

A CO_2 laser pulse of 12 to 15 µs in duration with various energies was focused onto the sample surface. The diameter of the laser beam on the flat samples was 15.5 mm.

2.1. Schlieren photography

The setup for the Schlieren pictures is illustrated in Fig. 1. The pulsed light source consisted of a frequency doubled Nd:YAG laser with a pulse length of 5-7 ns. The beam was enlarged by a telescope to a diameter of 10 cm. The light passed across the sample parallel to its surface and out of the vacuum tank on the opposite side. There it was refocused and sent through a 2 mm diameter orifice. The orifice not only cleaned up the picture from speckles, but also removed reflexes from beams bent in the density gradient field of the expanding ablation products. The orifice replaced the knife edge, conventional for Schlieren photography, in this fully 3 dimensional expansion. The expanding green laser beam was projected on a white paper screen and photographed from there with a digital camera.

For catching frames of the whole expansion process, the trigger unit allowed to delay the firing of the illumination laser such that it matched with the desired time after the start of the ablation process.

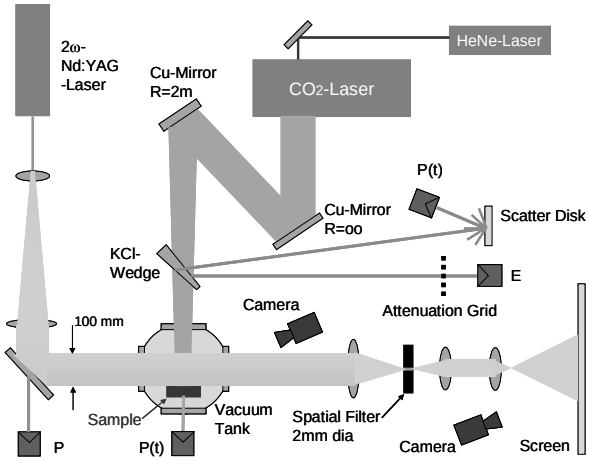

Fig. 1. Setup for the Schlieren Photography.

Since the blown-off material was not dense enough to become visible in the pictures with a vacuum below 1 mbar, the pressure in the tank was raised to approximately 35 mbar. This pressure is expected to be still low enough to be neglected as a counterforce for the expansion process. Nevertheless, the initial ablation motion releases a semi-spherical shock wave into the surrounding air that can be seen in the Schlieren pictures. The velocity of the shock wave can be determined from a sequence of pictures with various time delays. No velocity in the process can be greater than the shock velocity. Otherwise, a new shock wave would be released. Using 1-dimensional shock relations as an approximation, the material velocity and the thermodynamic state immediately behind the shock wave can be calculated. It is expected, that the velocity of the contact front is the same as that of the material boundary in vacuum.

2.2. Time dependant absorption measurement

The Schlieren pictures visualized the expansion process of the ablation products in the visible light. If the absorption in the plasma is strong enough it can also be seen. The question is now, where will the CO_2 radiation of the pulse laser be absorbed predominantly? This was attempted to be measured by a time resolved observation of the attenuation of continuous CO_2 laser beams across the expansion zone. Since no picture producing camera for the CO_2 wavelength has been available, only a point wise absorption measurement was possible. The CO_2 probe laser beam was not expanded but slightly focused by a lens with a long focal length of 500 mm. The focus had a diameter of approximately 2 mm and was placed on the central axes of the expansion cloud. At first it was attempted to split the probe laser beam into 4

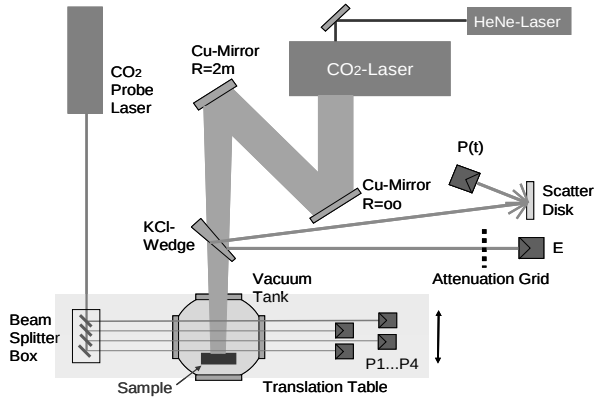

Fig. 2. Initial setup for the absorption measurement with 4 probe beams.

individual and parallel beams by semi-transparent mirrors and use 4 independent fast detectors for measuring the timely behavior of the arriving power. However, with a cw power of the CO_2 probe laser of 1 mW the individual beams were too weak for a discrimination against the infrared background of the plasma radiation. So the idea of using 4 parallel probe beams simultaneously was discarded and instead only 1 beam was used. Beam and detector were translated from shot to shot along the expansion axis. A bending mirror and a focusing lens on one side of the ablation zone and a re-focusing lens for placing the probe beam into the power meter on the other side were mounted on a common table. So, the whole optic could be moved simultaneously without realignment of the receiver. In the same way as for the Schlieren photography, the probe beams were transmitted through the vacuum tank with the ablation sample. Fig. 2 is a schematic of the initial setup with 4 beams. The beginning of the sampling was triggered by the electromagnetic noise pulse of the spark gap for the ignition of the CO_2 pulse laser.

A certain danger for the interpretation of the results was the possibility of a bending of the probe beam out of the detector by strong density gradients. This would pretend an absorption. Therefore, experiments have been carried out with a deliberate offset of the detector from the actual target point. If a bending would have taken place it should have been discovered by an eventual detector signal from the momentarily displaced beam. This did not happen, either because there was no bending or the absorption prevented the signal of a bent beam.

3. RESULTS AND INTERPRETATION

3.1. Energy absorption

Preliminary measurements of the energy transmitted through the absorbing ablation products and the ablation sample via a 3 mm hole on the axis of the pulse laser beam [3] have been extended to a broader range of material conditions and pulse energies. The assumption that the initial peak of the power curve after 300 ns is not yet influenced by the absorption mechanism gives the possibility to match the different scales of the power curve of the incident with the transmitted beam. The integration of both curves yields a non-calibrated, but directly comparable value for the accumulated energy. Therefore, the transmission ratio due to absorption, $R_t = E_{trans} / E_L$, can be directly inferred. E_{trans} is the energy measured behind the target and E_L is the incident laser pulse energy. The result is plotted in Fig. 3.

The smoothness of the data course with the laser pulse energy and the scatter of a few repeated measurements gives some confidence into the derived values, in particular with respect to the scale matching of the power curves. It is striking that the ablation of plain POM in vacuum leads to much less absorption (about 35% transmission in the limit of very high incident pulse energies) compared to the other cases: POM in atmospheric air and POM blended with aluminum powder. In these latter cases less than 10% (!) of the incident pulse energy actually arrive at the target surface in the limit of high pulse energies. A closer inspection of the data course indicates a linear dependence of the transmitted energy ration R_t on the inverse of the pulse energy E_L.

Another interesting result is the observed shortening of the transmitted laser pulse (Fig. 4). For POM in vacuum a maximum pulse length is found for the pulse energy of 120 J. The increase in pulse length for lower energies is

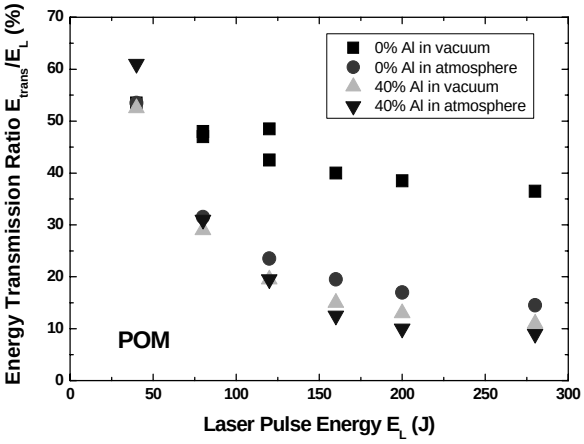

Fig. 3. Fraction of energy transmitted to the target surface.

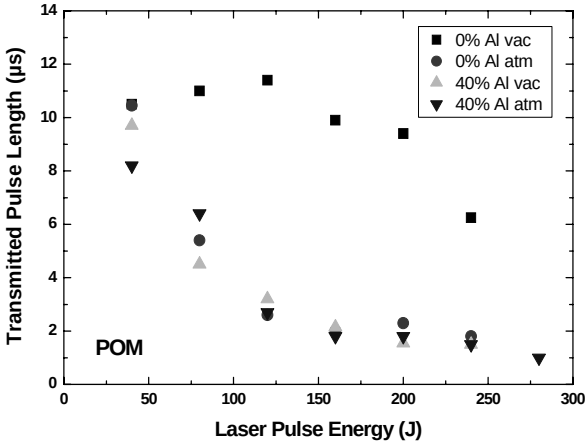

Fig. 4. Length of laser pulse transmitted to the target surface.

associated with the general increase of the incident laser pulse length with the pulse energy from about 10 µs at the low energies to over 12 µs at the higher energies. Above 120 J, the pulse length decreases rapidly, because the effect of pulse shortening by plasma absorption is now taking over. For the other 3 cases the pulse shortening is so strong from the very beginning that no optimum is found anymore. The transmitted pulse duration drops to as low as 1 µs. Finally, only the energy of the initial spike of the power curve arrives at the target.

3.2. Schlieren photography

Schlieren picture series have been made of plain POM for the following conditions:

Pressure	below 0.5 mbar,		35 mbar
Pulse energy	25 J,	75 J,	150 J
corresp. fluence	13 J/cm^2,	37 J/cm^2,	75 J/cm^2

For illustrating the different behavior, a picture series at the same pressures and with pulse energies of 75 J and 150 J has been made for POM with 20% Al also.

Typical Schlieren pictures are shown in Fig 5. Close to the target plane the pictures are obscured by the target fixture. Therefore, the plasma development cannot be seen during the first microsecond, corresponding to a maximum distance of ~3 mm. The saw tooth like structure at the bottom of the pictures is a scale with centimeter separation of the kerfs.

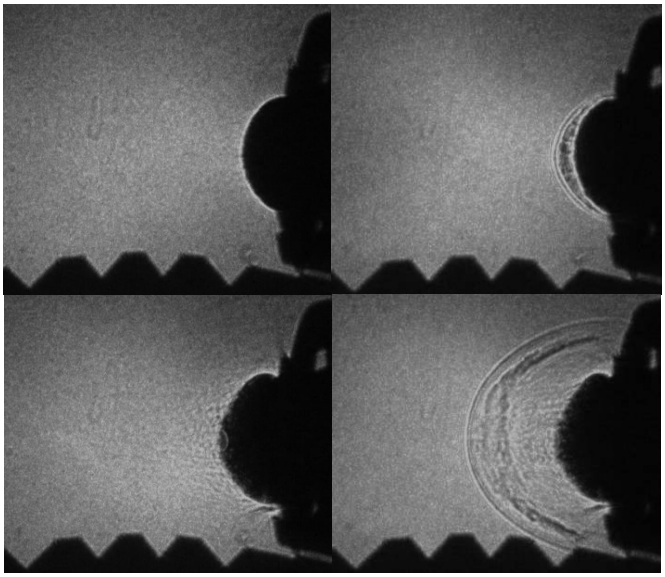

Fig. 5. Typical Schlieren Pictures at a pulse energy of 150 J; t = 2.6µs and t = 8.7 µs. (left hand side POM @ 0 mbar, right hand side POM @ 35 mbar).

3.2.1. POM

For both pressures a black ellipsoidal plume develops rapidly and reaches a maximum extension of 10 to 12 mm (energy dependent) after approximately 6 µs. This is the time when the laser pulse has reached its maximum power, too. Within 1 mm, the extension of the plume is equal for both pressure cases. The black plume is interpreted as the ablation plasma, which has an electron density high enough to absorb the illuminating light. The boundary is of remarkable sharpness. In the low pressure air, the detachment of a spherical shock from the plasma can be seen right after the appearance of the plasma. Several waves and a darker and a brighter zone follow the shock wave at nearly equal distances. The origin of these wakes is not known. However, when watching the picture series backwards, it appears likely that the transition from a brighter zone to a darker zone marks the contact front, the boundary between the off-flowing ablation products and the shocked air (darker zone).

When the laser pulse begins to decay after 8 to 9 µs, the sharp boundary of the plasma decays also and streamers in the flow direction become visible. Prominent vanes appear at the lower and upper boundary of the plasma. These could be artifacts from flow distortions at the screw heads that penetrate into the open space and obstruct a radial expansion. The streamers can be seen even after pulse termination, indicating that a vapor flow from the surface continues for some time, until the sample has cooled enough. After termination of the laser pulse, the contact line also seems to sharpen up. For a pulse energy of 150 J the bright/dark transition disappears after 6 µs and reappears after 11 µs. The line has moved out of the field of view after 25 µs.

3.2.2. POM + 20% Al

A sample with a 20% concentration of aluminum powder has been observed as well. In PVN samples with an additive, Urech et al. have observed a strange phenomenon (Ref. 6): The additive seems to expand with a higher velocity and to break through the shock wave. At a first glance this is physically impossible, because the penetrating material would launch another, even faster shock wave into the environment. We wanted to check this observation for our conditions with pulse energies of 75 J and 150 J.

It turned out that we could observe the same phenomenon indeed for the POM sample with Al: At a pulse energy of 75 J the creation of a new, non-uniform cloud is noticed for the first time after 4.7 µs. Already 1 µs later it has reached the initial shock front and after 9 µs it starts to bulge out the shock front. Another 2 µs later it has moved almost twice as far as the initial shock front and an entirely hemispherical front develops. In vacuum, this front can be seen equally well but does show a more irregular shape with local sub-centers. The plasma front is less well defined as in the previous experiments with plain POM and seems to extend not as far as for plain POM. Remarkable is also the disappearance of the Schlieren, at first in vacuum between 11.5 µs and 15.7 µs and thereafter in air, leaving just a diffuse cloud near the target surface with probably still evaporating material. At the pulse energy of 150 J the same phenomenon happens at an earlier time. Already after 3.7 µs the second cloud has reached the shock front and has penetrated through it during the next microsecond. While in the low pressure environment the ejected material remains confined within a sharply bound front, in vacuum it spreads out diffusively in all directions. Apparently, the residual air still exerts a drag force on the ejected matter. In air, the ejection turns into an almost one-dimensional process. Between 8 and 9 µs the ejected matter leaves the field of view.

3.3. Velocity of the ablation products

The series of Schlieren pictures allows the direct measurement of various velocities: shock wave, plasma expansion and with some caution the velocity of the contact front, which would represent the maximum ablation velocity. The data from the pictures have been collected in diagrams of the front positions versus time. Typical diagrams are shown in Fig. 6 and 7 for POM and for doped POM, respectively. Also displayed in the diagrams are the power curves at comparable energetic conditions. The dashed line at 3 mm distance from the target marks the distance, where a feature can be discovered for the first time. The first data point location is therefore not exact and the true location of the surface is not known to better than 1 mm. However, all distances relative to each other are precise to within a fraction of a millimeter. The shock front and the contact front show a linear behavior and thus possess a unique speed for a fixed energy. Yet, the shock speed grows with the pulse energy. But, while the pulse energy is increased 6-fold from 25 J to 150 J, the shock velocity only goes up from 2 km/s to 2.5 km/s. It is not expected that the ablation velocity in vacuum is significantly different from the velocity of the contact front, as interpreted from the pictures in low pressure air. This is very different though for the doped material, for which the ablation products assume a much higher front velocity for the pulse energy of 150 J: over 8 km/s.

It is surprising that the velocities of the shock and contact front are constant over time. This is expected for a one-dimensional expansion only. For multi-dimensional expansion one would expect a slow-down of the velocity with time, because the driving energy dissipates in several directions. The measured velocities of the potential contact surface are 1500; 1925; and 2275 m/s.

As the pulse energy is increased, the isentropic coefficient should be reduced to less than 1.3, which seems

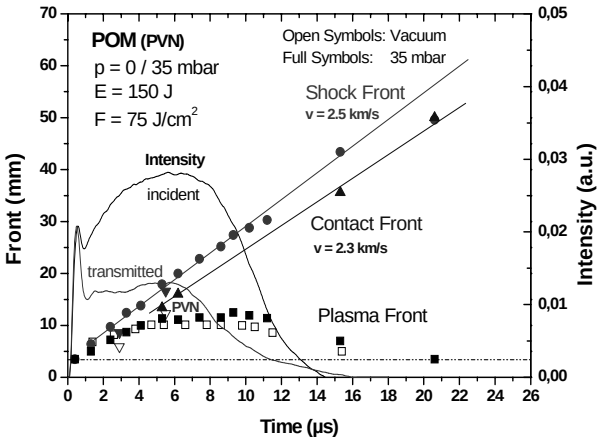

Fig. 6. Space/time diagram of the shock and contact front for a pulse energy of 150 J in comparison with the intensity curve. Target material: POM.

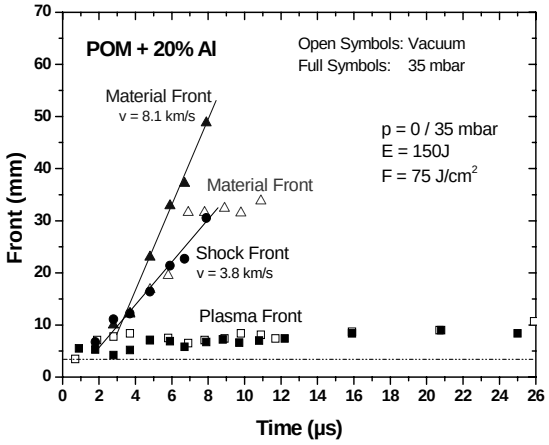

Fig. 7. Space/time diagram of the shock and contact front for a pulse energy of 150 J in comparison with the intensity curve. Target material: POM + 20% Al.

reasonable. It is remarkable that the pressure behind the shock wave in the disturbed air rises to over 1 bar and the temperatures reach values up 2500 K.

While in the case of plain POM the radiation penetrates into the material according to the optical transmission, decomposes the chemical structure, and vaporizes the products, it is conceivable that with the larger concentrations of optically dense materials, like metals, a different process takes place. One explanation could be that the metal grains act as scattering objects that guide light to some depth. Interference may lead to local energy concentrations. The polymer with its low decomposition temperature goes into a gaseous state and builds up a pressure that is finally capable to eject the metal grains with very high speed like in a cannon. This process would have some similarity with a confined ablation (Refs. 7 and 8).

3.4. Absorption measurements

With the absorption measurement setup it was possible to scan the zone for 10.6 µm absorption in front of the target and look at the temporal development of the absorption fraction. Two major problems made the evaluation of the measurements difficult: 1) The continuous plasma radiation was very strong around the CO_2 band compared to the probe laser beam intensity and could not be totally suppressed. However, increasing the distance of the power meter from the radiation source reduced the background to an acceptable level. The signal was still very noisy. 2) As the probe beam is moved away from the sample surface and due to the finite expansion velocity of the ablation cloud, the onset of absorption must be delayed in proportion to the distance. This was the case in general. Absorption measurements were carried out for pulse energies of 150 J, 75 J and 25 J in vacuum and also for 150 J in ambient air of 30 mbar.

As a function of time after the beginning of the laser pulse, Fig. 8 shows the power traces of the partially absorbed probe beam for various distances from the target surface. For comparison, the power trace of the pulse of the ablation laser is also included in the diagram ("incident power"). The measurements shown in this diagram have been made for

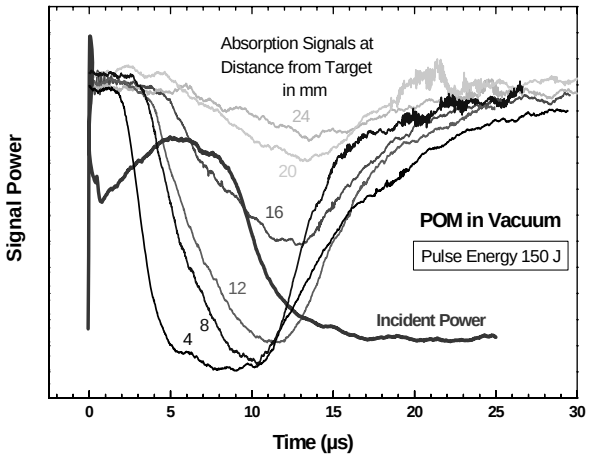

Fig. 8. Temporal development of the CO_2 wavelength absorption at various distances from target surface for a pulse energy of 150 J.

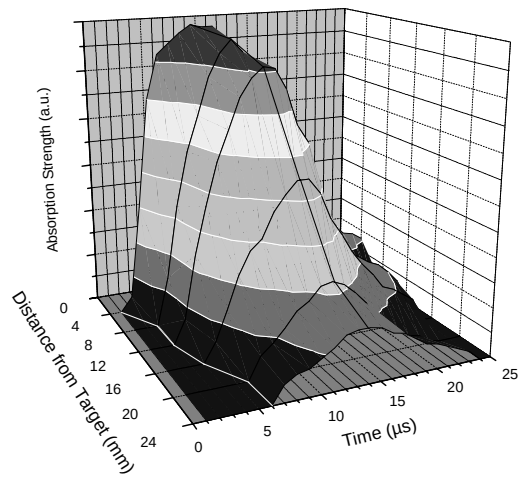

Fig. 9. 3-dimensional representation of the absorption wave.

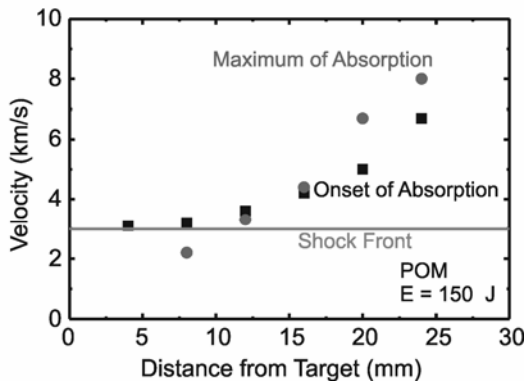

Fig. 10. Velocity of shock and absorption waves.

POM in vacuum with a pulse energy of 150 J. The resolution in location is comparable to the diameter of the probe beam at the location of the measurement. For the presented results this is 2 mm. Due to the finite angular resolution of the setup, plasma radiation from upstream regions may be seen before absorbing media cross the probe beam. The absorption is strongest near the target and decreases with the distance. The absorption also lives longest near the target where plasma recombination is delayed by lasting high temperatures. Fig. 9 is a 3 D re-plot of the absorption region in space and time, with the absorption strength in vertical direction. Note: The magnitude of the absorption for different time traces is arbitrary. The diagrams are only to show the extension and motion of the absorption region in the space-time domain.

The surprising result of these measurements is (1) the high, and (2) an even strongly accelerating velocity of both, the onset of the absorption (> 3 km/s) and the attaining of the absorption maximum (> 2 km/s). The result does not correspond to the findings with the Schlieren observations, where a constant material velocity (contact front) of 2.3 km/s to distances of 50 mm from the target has been found (Fig. 10). Absorbing matter would have to expand much faster than can be seen in the Schlieren pictures. What kind of matter could that be and where does it come from? If some available matter is postulated, at least the increasing acceleration could be explained in terms of a detonation wave with a constant heating in the region immediately behind the front. But a detonation wave, precursing the shock wave should be visible in the Schlieren pictures.

3.5. Abnormal absorption

Abnormal absorption is understood as the absorption that starts immediately with the laser pulse (Fig. 11). We have attempted to find the reason for this as yet unidentified phenomenon by procedures described below. The only natural explanation is a breakdown independent of the target. Such a breakdown can happen in a gas with a low breakdown threshold, for instance in residual air, possibly contaminated with products of the previous ablation shot. Although the vacuum pump is running continuously, this seems conceivable, if some dust that has settled down on the tank wall is whirled up again by an ablation shot. Also, floating dust may not settle down for a long time. In addition, the local intensity in front of the target may be enhanced by reflections from the target. The hypothesis that residual air might trigger a premature breakdown is not supported though by the measurements with 30 mbars of background air. No early breakdown was found in these measurements.

Nevertheless, a series of individual tests have been performed to rule out more or less obvious causes. For these tests, the probe beam was placed 6 mm in front of the target. The pulse energy was always kept at 150 J. Some of the results are displayed in figure 11.

1) The presence of residual air or other contamination products has been reduced by extended pumping before the next shot (1/2 hour with a final pressure < 0.05 mbar). Abnormal absorption was observed anyway (Fig. 11, curve # 4).

2) Careful cleaning of the tank and purging with dry nitrogen did not prevent the abnormal absorption.

3) Artificial contamination has been attempted by blowing nitrogen across the target surface. This raised also the pressure in the tank. The abnormal absorption was not enforced.

4) Puffs of gas into the tank before a shot to whirl up any settled down contamination did not result in abnormal absorption (curve # 2).

5) Continuous flushing at a distance of 5 cm from the target surface (curve # 1) and at 1 cm (curve # 3) gave ambiguous results.

6) After the complete removal of target and target holder no absorption was found at all.

7) Replacing the polymer target by a target of sandblasted aluminum resulted in a very bright plasma

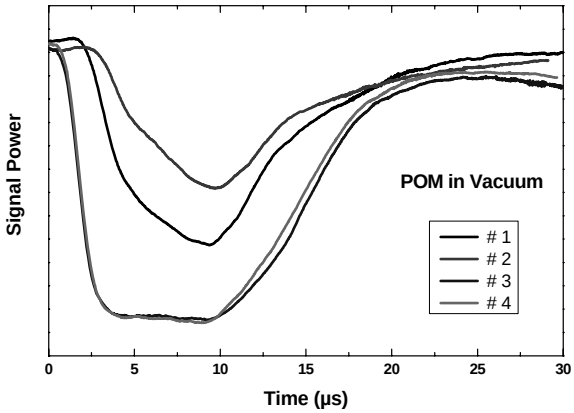

Fig. 11. Comparison of normal and abnormal absorption curves for different experimental conditions. (# 1: continuous flushing 5 cm from sample surface; # 2: flushing 5 cm from sample surface, then pulse after some delay; # 3: continuous flushing 1 cm from sample surface; # 4: no flushing, pressure < 0.05 mbar).

and an initially strong absorption. This absorption, however, decreased with every consecutive shot and is thus contributed to surface contamination of the sample.

8) The effect of a deflection of the probe beam by the expanding gas has been checked once more and none was found.

9) A possible interference of electromagnetic radiation with the detector has been ruled out by successively covering up all optical radiation.

10) In the same way, scattering by secondary reflections of the ablation laser pulse into the detector has been ruled out.

11) Finally, it has been checked if the laser emits a prepulse that had remained undetected by the applied trigger method. No such pulse was found that could have released a small amount of matter from target before the main pulse was applied.

All these tests led to no concise conclusion on the origin of the abnormal absorption and how to prevent it. Other explanations, like very fast precursor electrons from the target plasma, can probably be ruled out because of the build-up of a space charge. But the ions would follow not faster than the shock wave expands and hold the electrons back. Also, such a process should occur for every shot.

4. CONCLUSION

It was found that the fraction of energy that is not absorbed in front of the target surface is inversely proportional to the applied pulse energy. The length of the penetrating energy pulse is also shortened with increasing pulse energy. In the limit, only the initial spike energy can penetrate to the target surface.

In the experiments employing Schlieren Photography with nanosecond exposure times we could show the formation of a surface plasma along with the deposition of energy into a target sample. The plasma expands to a maximum distance of 12 mm from the surface. In a gaseous environment the plasma expansion launches a strong shock wave with Mach no. ~6. From the velocity of the shock wave and the assumption of a quasi one-dimensional expansion process, an approximate expansion velocity of the material cloud of ablation products can be deduced. As the released gas or vapor expands, an absorption wave spreads out. This is, where most of the incident pulse power is subsequently absorbed. The addition of heat into the off-flowing matter can be one reason why the velocity, observed as the shock velocity, does not decrease over an extended time, as would be expected for a multi-dimensional expansion. The circular shape of the density gradients, as seen in the Schlieren pictures, does suggest a 3-dimensional expansion, although probably not in the full half-space. Shock velocities in the range of the applied pulse energies of 150 J (fluence 75 J/cm^2) were not higher than 2.5 km/s for plain POM. Only POM samples blended with a certain amount of metal powder showed an unusual behavior with material escape velocities in excess of 8 km/s. Since such high material speeds did not result in improved generation of the mechanical impulse, these very interesting findings deserve some more investigations of fundamental nature.

Position and time resolved measurements of the absorption cloud itself have been made in the same parameter regime as the optical Schlieren observations, using a CO_2 probe laser beam transversely through the expanding cloud. Surprisingly, the measured absorption wave generally expands much faster than the optically measured velocity of the shock wave. Furthermore, the velocity of the onset of absorption increases in time at a constant rate. No correspondence between the material expansion and the absorption wave could be made out. We are left with the unsatisfactory circumstances that two processes have been observed with different expansion behavior that could not be brought into an at least close agreement. The explanation for the absorption, which is so important for the achievement of high impulses in ablation propulsion, thus remains still an open question.

It had been claimed that the applied CO_2 laser pulse, consisting of two peaks, simulates a double pulse arrangement. In the double pulse arrangement a first pulse releases some matter from the target into which a second, stronger pulse is placed. The resulting shock wave that travels backwards towards the target should give rise to a pressure jump and hence an impulse at the target surface. However, the Schlieren pictures show a fairly continuous motion in one direction only. There is no indication of a wave traveling backwards towards the target surface. Therefore, no retrograde build-up of pressure is expected as a result of a second shock wave. The application of the double pulse effect would require two independent pulses, in which the heating process from the first pulse is completely terminated before the second pulse arrives.

In summary, we must conclude from the results, that a CO_2 laser with pulse lengths of several microseconds in combination with polymers as propellant is not an ideal laser for beamed energy propulsion. The pulse length should be

much shorter than the characteristic time for the build-up of an absorption wave, which is less than 1 µs. Energy that is absorbed in such an absorption zone serves only to increase the expansion rate of the zone itself and has no effect back on the target. Pulsed laser ablation rockets, that gain their momentum only from the release of matter directly at the target surface probably work only efficiently for either low energy pulses at a relatively high pulse rate (kHz) or with sub-microsecond pulse lengths. For pulsed high-power CO_2 lasers these conditions are not easy to achieve and require special development efforts.

Unfortunately, the true nature of the absorbing media could not be unveiled, since no coincidence between the absorption measurements and the flow visualization could be made out. It was the promise that the knowledge about the absorption mechanism could lead to a design where the absorbing medium can be confined in some kind of thrust chamber, like those of conventional rockets. Then, a pressure would build up and produce an additional momentum. In the limit this would lead to the continuous laser rocket. Now, future research with new methods of investigation must lead to a better understanding of the absorption phenomenon and its coupling to the ablation process.

ACKNOWLEDGMENTS

Part of this research has been supported by the EOARD, London under the contract number FA 8655-04-1-3067. The authors are grateful to Dr. Frank Mead, Dr. Carl W. Larson and Dr. Ingrid Wysong for the initial support of this project. We also thank Dr. Thomas Lippert for interesting discussions and the supply of samples of new polymer compounds.

REFERENCES

1. W.O. Schall et.al., “Comparative lightcraft impulse measurements”, High Power Laser Ablation IV, Proc. SPIE Vol. 4760 (2002) 908.
2. W.O. Schall et.al., “Ablation Performance Experiments with Metal Seeded Polymers“, ISBEP3, AIP Conf. Proc. 766 (2005)
3. W.O. Schall, H.-A. Eckel, J. Tegel, F. Waiblinger, S. Walther, “Properties of Laser Ablation Products of Delrin with CO2 Laser”, EOARD Grant FA8655-03-1-3061, Final Report, May 2004.
4. C.R. Phipps and J. Luke, ”Micro laser plasma thrusters for small satellites”, High Power Laser Ablation III, Proc. of SPIE Vol. 4065 (2000) p.801-809..
5. D.A. Reilly, “Laser Propulsion Experiments - Final Report”, AVCO Research Lab, Inc., Everett, Maine 02149, Subcontract B116822 for University of California Livermore National Laboratory, Jordan Kare, Program Manager (1991).
6. L. Urech, M. Hauer, T. Lippert, C.R. Phipps, E. Schmid, A. Wokaun, I. Wysong, ”Designed polymers for laser-based microthrusters: correlation of thrust with material, plasma, and shockwave properties”, High Power Laser Ablation V, Proc. SPIE Vol. 5448 (2004) p.52-64..
7. K. Mori, K. Watanabe, A. Sasoh, “Large impulse launch using 300-J CO2 TEA Laser”, ISBEP3, AIP Conf. Proc. 766 (2005), p.385-393.
8. R. Fabbro, J. Fournier, P. Ballard, D. Devaux, J. Virmont, ”Physical Study of Laser-produced Plasma in Confined Geometry”, J.Appl.Phys. Vol.68, No.2 (1990) p.775-784A. Eisenberg, *Guide to Technical Editing*, Oxford University, New York, 1992.